D-mannose facilitates immunotherapy and radiotherapy of triple-negative breast cancer via degradation of PD-L1

Ruonan Zhang[a] [iD], Yajing Yang[a] [iD], Wenjing Dong[a], Mingen Lin[a] [iD], Jing He[a], Xinchao Zhang[a], Tongguan Tian[b] [iD], Yunlong Yang[c] [iD], Kun Chen[d], Qun-Ying Lei[e], Song Zhang[f,1] [iD], Yanping Xu[b,1] [iD], and Lei Lv[a,1]

[a]Ministry of Education Key Laboratory of Metabolism and Molecular Medicine, Department of Biochemistry and Molecular Biology, School of Basic Medical Sciences, Fudan University, Shanghai 200032, China; [b]Tongji Hospital, Shanghai Key Laboratory of Signaling and Disease Research, Frontier Science Center for Stem Cell Research, School of Life Sciences and Technology, Tongji University, Shanghai 200120, China; [c]Department of Cellular and Genetic Medicine, School of Basic Medical Sciences, Fudan University, Shanghai 200032, China; [d]Translational Medical Center for Stem Cell Therapy and Institute for Regenerative Medicine, Translational Medical Center for Stem Cell Therapy, Shanghai East Hospital, School of Life Sciences and Technology, Tongji University, Shanghai 200120, China; [e]Fudan University Shanghai Cancer Center and Cancer Metabolism Laboratory, Institutes of Biomedical Sciences, Shanghai Medical College, Fudan University, Shanghai 200032, China; and [f]Institute for Immunology and College of Life Sciences, Nankai University, Tianjin 300071, China

Breast cancer is the most frequent malignancy in women worldwide, and triple-negative breast cancer (TNBC) patients have the worst prognosis and highest risk of recurrence. The therapeutic strategies for TNBC are limited. It is urgent to develop new methods to enhance the efficacy of TNBC treatment. Previous studies demonstrated that D-mannose, a hexose, can enhance chemotherapy in cancer and suppress the immunopathology of autoimmune diseases. Here, we show that D-mannose can significantly facilitate TNBC treatment via degradation of PD-L1. Specifically, D-mannose can activate AMP-activated protein kinase (AMPK) to phosphorylate PD-L1 at S195, which leads to abnormal glycosylation and proteasomal degradation of PD-L1. D-mannose–mediated PD-L1 degradation promotes T cell activation and T cell killing of tumor cells. The combination of D-mannose and PD-1 blockade therapy dramatically inhibits TNBC growth and extends the lifespan of tumor-bearing mice. Moreover, D-mannose–induced PD-L1 degradation also results in messenger RNA destabilization of DNA damage repair–related genes, thereby sensitizing breast cancer cells to ionizing radiation (IR) treatment and facilitating radiotherapy of TNBC in mice. Of note, the effective level of D-mannose can be easily achieved by oral administration in mice. Our study unveils a mechanism by which D-mannose targets PD-L1 for degradation and provides methods to facilitate immunotherapy and radiotherapy in TNBC. This function of D-mannose may be useful for clinical treatment of TNBC.

D-mannose | triple-negative breast cancer | PD-L1 | immunotherapy | radiotherapy

Breast cancer is the most common type of cancer in women all over the world and is curable in most early-stage, nonmetastatic patients (~70 to 80%) (1). Triple-negative breast cancer (TNBC), which is characterized by absence of the molecular markers estrogen receptor (ER), progesterone receptor (PR), and human epidermal growth factor receptor 2 (HER2) and accounts for ~15 to 20% of all breast cancer cases (2, 3), has the worst prognosis compared to other subtypes, and the 5-y survival rate for these women if they do not present with metastatic disease is 65 to 90% depending on the disease stage at diagnosis. TNBC is highly invasive and has the highest risk of distant metastasis (~46%) (1, 4). Notably, the median survival time of patients after metastasis is only 13.3 mo (4). The therapeutic strategies for TNBC are very limited. Until 2019, TNBC treatment was still restricted to chemotherapy (2). Over the past 2 y, immunotherapy, in combination with chemotherapy, has been applied in TNBC treatment and has shown promising results, but a large number of TNBC patients are nonresponsive or resistant to immunotherapy. In addition,

radiotherapy can also improve locoregional control of breast cancer. However, TNBC shows resistance to radiotherapy, and radiotherapy did not change the local recurrence rate of TNBC (5). Overall, TNBC treatment is still a challenge, and exploring appropriate systematic treatments and improving the efficacy of immunotherapy and radiotherapy are important goals of breast cancer research.

Programmed death ligand 1 (PD-L1, also called B7-H1) is a 33-kDa protein located either on the cell membrane or in the cytoplasm. Membrane-localized PD-L1 can inhibit the proliferation and cytolytic activity of T cells to help cancer cells escape from immune surveillance via interaction with its receptor programmed cell death protein 1 (PD-1) on immune cells (6, 7). Immune checkpoint blockade therapy has been a focus of cancer research and treatment in recent years (8). Immunotherapies targeting PD-1/PD-L1 have shown substantial clinical benefits in

Significance

PD-L1 is well known as an immune checkpoint molecule, which suppresses immune surveillance through binding to its receptor PD-1. Intracellular PD-L1 can also protect messenger RNAs of several DNA damage repair–related genes from degradation and enhance tumor resistance to DNA-damaging therapy. Triple-negative breast cancer (TNBC) has the worst prognosis and highest risk of distant relapse in breast cancer and shows resistance to immunotherapy and radiotherapy. In this study, we found that D-mannose can promote the degradation of PD-L1 and significantly enhance immunotherapy and radiotherapy of TNBC. Since TNBC treatment is still a clinical challenge, our findings provide strategies to enhance the therapeutic efficacy of TNBC and may have clinical application.

different tumor types (9, 10). In addition to its well-established role as an immune checkpoint molecule, intracellular PD-L1 also acts as an RNA-binding protein and competes with RNA exosomes to increase RNA stability globally. Specifically, PD-L1 in the cytoplasm binds with messenger RNAs (mRNAs) of several DNA damage repair (DDR)-related genes and protects them from degradation, which facilitates the DDR and enhances tumor resistance to DNA-damaging therapy (11).

Glycosylation is one of the most important posttranslational modifications (PTMs) (12). Glycans have been shown to play different biological roles in glycoproteins, such as assisting correct folding, targeting proteins to specific receptors, controlling the residence time in the bloodstream, and regulating the function of proteins (13). N-glycosylation is one of the most common glycosylation forms on proteins. N-linked glycans are covalently attached to proteins at the asparagine residue of the NXT motif (Asn-X-Ser/Thr) when the new proteins are being translated and transported into the endoplasmic reticulum. All N-glycans share a common core sequence and are further classified into three types: high D-mannose, hybrid, and complex glycans (14, 15). It has been reported that complex N-glycan exists on the extracellular domain of PD-L1 and that PD-L1 is N-glycosylated at N35, N192, N200, and N219 in cancer cells (16), which promotes its stability and suppresses T cell activity. Glycosylation of PD-L1 is also essential for the PD-L1/PD-1 interaction and immunosuppression in TNBC (17). Interestingly, metformin, a drug widely used for the treatment of type 2 diabetes, was reported to induce abnormal glycosylation and degradation of PD-L1 (18).

D-mannose, a C-2 epimer of glucose, is the major monosaccharide component of N-glycans and is internalized into mammalian cells via membrane glucose transporters (19). Once taken into cells, D-mannose is phosphorylated by hexokinase (HK) and produces mannose-6-phosphate (M6P), which can be directed into glycolysis or glycosylation pathway (20). Previous studies demonstrated that a supraphysiological level of D-mannose could enhance the sensitivity of cancer cells to chemotherapy (21) and suppress the immunopathology of autoimmune diabetes and airway inflammation (22). D-mannose has also been shown to oppose macrophage activation by impairing IL-1-β production (23). More recently, D-mannose was reported to suppresses oxidative response and block phagocytosis in experimental neuroinflammation (24). However, the function of D-mannose in immunotherapy and radiotherapy in cancer remains unknown. Here, we demonstrated that D-mannose can target PD-L1 for degradation by impairing its glycosylation via AMPK activation. Importantly, oral administration of D-mannose decreased PD-L1 levels in mice, which promoted antitumor immunity and sensitized TNBC to radiotherapy.

Results

D-mannose Decreases PD-L1 Protein Levels. As glycosylation can stabilize PD-L1 by protecting it from GSK3-β–mediated proteasomal degradation (16), we wondered whether different sugars have an impact on PD-L1 stabilization by interfering with its glycosylation. Therefore, we examined the effects of various hexoses on the protein level of PD-L1. Surprisingly, instead of stabilization, D-mannose significantly reduced PD-L1 protein levels (Fig. 1 *A* and *B*) but not mRNA levels (Fig. 1 *C* and *D*) in MDA-MB-231 and BT-549 cells. To confirm this result, we treated both cell lines with D-mannose for different times, and the results showed that the PD-L1 level was reduced in a time-dependent manner (Fig. 1 *E* and *F*). Similar effects occurred when cells were treated with increasing concentrations of D-mannose, and the expression of PD-L1 decreased in a dose-dependent manner in both cell lines (Fig. 1 *G* and *H*). Notably, in addition to decreasing its protein level, D-mannose

treatment also resulted in a band shift of PD-L1 (Fig. 1 *E* and *G*), suggesting D-mannose may impair but not promote glycosylation of PD-L1. To find out whether the effect of D-mannose on PD-L1 protein level is isomer specific, we treated MDA-MB-231 cells with either D-mannose or L-Mannose for 48 h and examined their effects on PD-L1. Result showed that L-mannose did not affect glycosylation and protein level of PD-L1, demonstrating that the function of D-mannose on PD-L1 regulation is isomer specific (*SI Appendix*, Fig. S1*A*). Moreover, we examined the effect of D-mannose on the PD-L1 expression on cell surface by measuring cell surface PD-L1 level via flow cytometry under D-mannose treatment. Results showed that D-mannose significantly decreases cell surface PD-L1 levels in both MDA-MB-231 and BT-549 cells (Fig. 1 *I* and *J*). Together, these results demonstrate that D-mannose can significantly decrease PD-L1 protein levels in TNBC cells.

Given that high level of glucose may compete with D-mannose for glucose transporter to import into the cells, we examined the effects of glucose depletion and low concentrations of glucose on D-mannose–induced down-regulation of PD-L1. Results showed that both glucose depletion and decreasing glucose concentration enhanced the ability of D-mannose to decrease PD-L1 (Fig. 1 *K* and *L*). As a glucose analog, 2-DG was reported to block PD-L1 glycosylation and decrease its stability (25), we treated cells with 2-DG and examined the PD-L1 level. Interestingly, 2-DG synergized the effect of D-mannose on reducing PD-L1 level (Fig. 1*M*). These findings raised the question whether glucose modulation is sufficient to have an effect on PD-L1 level. We examined the effects of glucose modulation on PD-L1 level. Results showed that both inhibition of glucose transporter 1 (GLUT1) with WZB117 and down-regulation of glucose concentration slightly reduced PD-L1 protein levels in MDA-MB-231 and BT-549 cells (*SI Appendix*, Fig. S1 *B–E*). Both the effects were minor and showed no band shift of PD-L1, which was quite different from D-mannose treatment, indicating impaired glucose metabolism and D-mannose treatment induced down-regulation of PD-L1 may be separate. Furthermore, we examined the levels of glycolytic metabolites in control and D-mannose–treated MDA-MB-231 cells. Surprisingly, the levels of glycolytic metabolites were much higher in D-mannose–treated cells than control cells (*SI Appendix*, Fig. S1*F*). According to previous studies (21, 23), the susceptibility of tumor cells to D-mannose was dictated by the expression level of phosphomannose isomerase (PMI), which catalyzes the interconversion of M6P and fructose-6-phosphate (F6P) and helps cells to utilize the D-mannose as a fuel of glycolysis. D-mannose–mediated glycolysis inhibition has been reported in U2OS cells and macrophages, both of which possess low PMI levels. When treated with D-mannose, M6P is accumulated in those PMI-low cells and inhibits the activity of glycolytic enzymes HK and phosphoglucose isomerase (PGI), thus impairing glycolysis (*SI Appendix*, Fig. S1 *G*, *Middle*) (21). However, MDA-MB-231 cells were reported to show high levels of PMI (21, 23). In our study, MDA-MB-231 cells were treated for 72 h with supraphysiological level of D-mannose, which was converted to M6P and then to F6P by high level of PMI to fuel glycolysis (*SI Appendix*, Fig. S1 *G*, *Right*). Together, these results demonstrate that D-mannose does not induce PD-L1 down-regulation through impairing glucose metabolism.

D-mannose Disturbs PD-L1 Glycosylation and Stabilization by Activating AMPK. We next determined whether D-mannose decreases PD-L1 by impairing its stability. Indeed, in the presence of cycloheximide, a protein synthesis inhibitor, the turnover rate of overexpressed PD-L1 under D-mannose treatment was much faster than that of the control in 293T cells (Fig. 2*A*). Similar results were observed in MDA-MB-231 cells with endogenous PD-L1 expression (Fig. 2*B*). To determine how PD-L1 was degraded, we treated MDA-MB-231 cells with
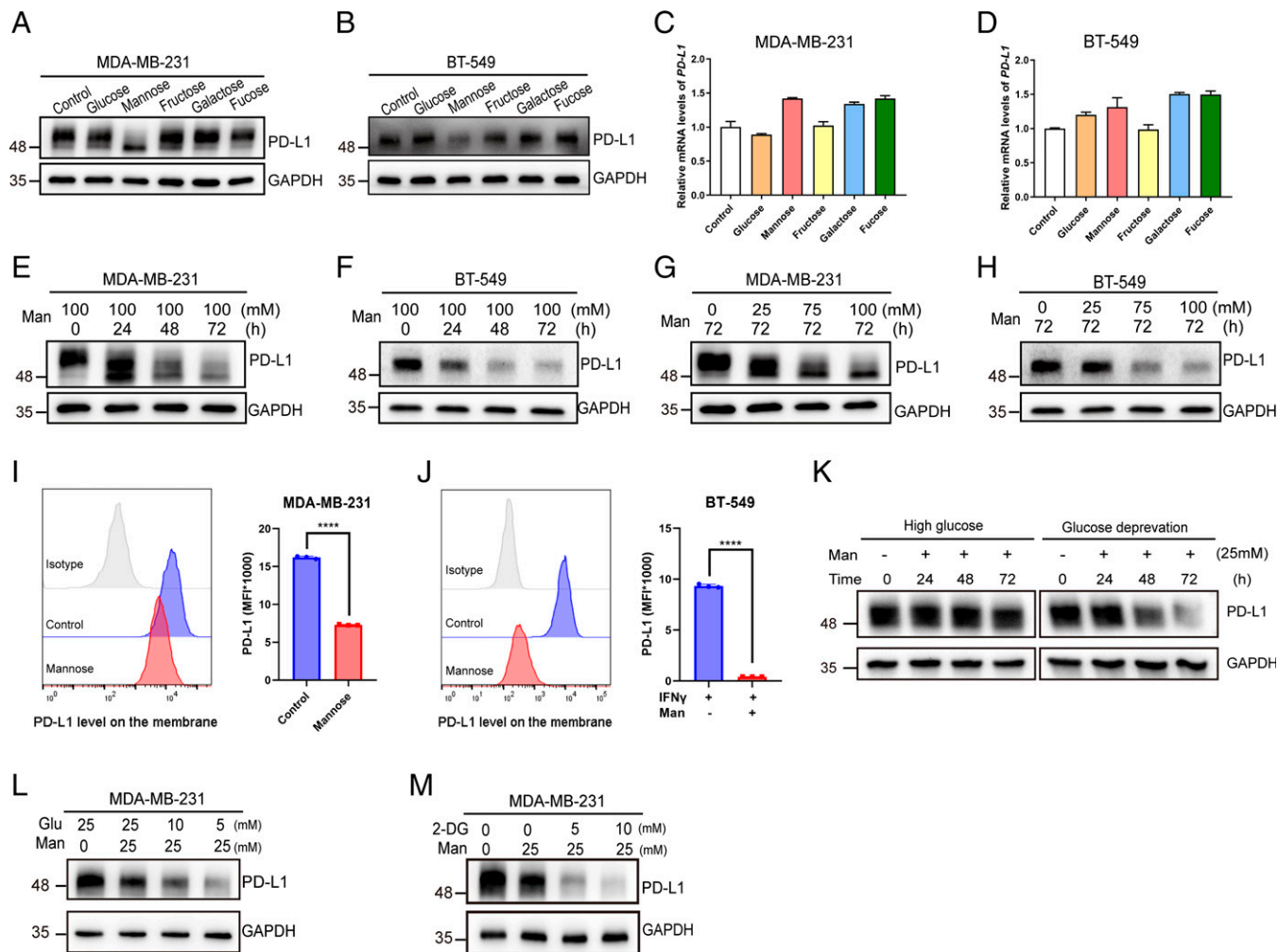
Fig. 1. D-mannose down-regulates PD-L1 in TNBC cells. (*A* and *B*) Western blot analysis of PD-L1 level in MDA-MB-231 cells (*A*) and BT-549 cells (*B*) treated with or without different hexoses as indicated. (*C* and *D*) qRT-PCR analysis of PD-L1 level in MDA-MB-231 cells (*C*) and BT-549 cells (*D*) treated with or without different hexoses as indicated. Values are means ± SD from $n = 3$ independent experiments. (*E* and *F*) Western blot analysis of PD-L1 level in MDA-MB-231 cells (*E*) and BT-549 cells (*F*) treated with 100 mM D-mannose for different time as indicated. (*G* and *H*) Western blot analysis of PD-L1 level in MDA-MB-231 cells (*G*) and BT-549 cells (*H*) treated with different concentrations of D-mannose as indicated for 72 h. (*I* and *J*) Flow cytometry analysis of membrane PD-L1 expression in MDA-MB-231 (*I*) and BT-549 cells (*J*) (stimulated with IFN-γ under D-mannose treatment. Representative histograms and summarized mean fluorescent intensity (MFI) are shown. Values are means ± SD from $n = 3$ independent experiments. Statistical differences were determined by Student's *t* test. ****$P < 0.0001$. (*K*) Western blot analysis of PD-L1 level in MDA-MB-231 cells treated with 25 mM D-mannose for different time under high glucose or glucose deprivation. (*L*) Western blot analysis of PD-L1 level in MDA-MB-231 cells treated with 25 mM D-mannose and decreasing concentrations of glucose as indicated for 72 h. (*M*) Western blot analysis of PD-L1 in MDA-MB-231 cells treated with 25 mM D-mannose and increasing concentrations of 2-DG as indicated for 72 h.

MG132, NH$_4$Cl, and 3-MA, which inhibit protein degradation through the proteasome, lysosome, and autophagy pathways, respectively, in the presence of D-mannose. The results demonstrated that only MG132 could rescue D-mannose–induced degradation of PD-L1, indicating that D-mannose may reduce PD-L1 via proteasomal degradation (Fig. 2*C*). To confirm this hypothesis, we examined the ubiquitination level of PD-L1 under D-mannose treatment and found that ubiquitination of PD-L1 was substantially increased by D-mannose (Fig. 2*D*). Collectively, D-mannose promoted the ubiquitination of PD-L1 and targeted it to the proteasome for degradation. Notably, D-mannose treatment–induced band shift of PD-L1 could not be rescued by MG132 treatment (Fig. 2*C*). Previously, a similar band shift was observed and attributed to an abnormal glycan structure, which destabilized PD-L1 (18). Taken together, these results suggest that D-mannose may decrease PD-L1 levels by interfering with its glycosylation. To determine which glycosylation site is responsible for D-mannose–induced PD-L1

degradation, we mutated four glycosylation sites of PD-L1 in 293T cells that were reported to affect PD-L1 stability (16). Surprisingly, the levels of wild-type (WT) and the N35Q, N192Q, N200Q, and N219Q PD-L1 mutants all decreased under D-mannose treatment (Fig. 2*E*), while the 4NQ mutant, in which PD-L1 glycosylation was completely ablated, showed no response to D-mannose treatment (Fig. 2*E*). These results suggest that D-mannose down-regulates PD-L1 by impairing its glycosylation.

We next attempted to illustrate how D-mannose impairs PD-L1 glycosylation. Previous study reported that AMPK-mediated phosphorylation of PD-L1 impairs its glycosylation and stabilization, suggesting that AMPK may also play a role in D-mannose–induced abnormal glycosylation and destabilization of PD-L1 (18). To test this hypothesis, we first examined the phosphorylation level of AMPK under D-mannose treatment. The results showed that the activation of AMPK was positively correlated with the band shift of PD-L1 and negatively
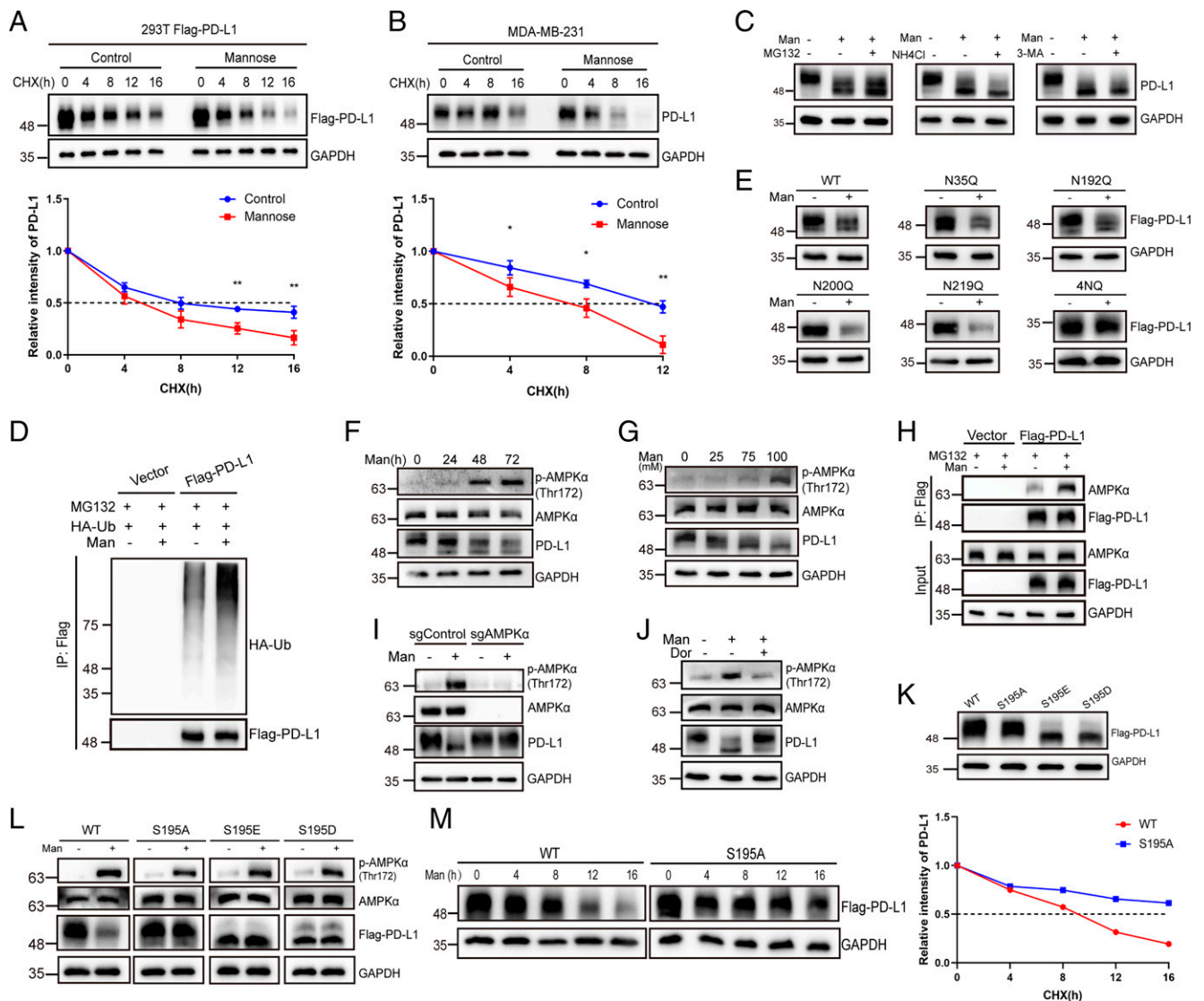
Fig. 2. D-mannose disturbs PD-L1 glycosylation and stabilization through activating AMPK. (*A* and *B*) The half-life of PD-L1 under D-mannose treatment was determined by cycloheximide (CHX)-chase assay in 293T cells overexpressed with PD-L1 (*A*) and MDA-MB-231 cells (*B*). The quantifications are shown below. Values are means ± SD from $n = 3$ independent experiments. Statistical differences were determined by Student's *t* test. *$P < 0.05$, **$P < 0.01$. (*C*) Western blot analysis of PD-L1 level in MDA-MB-231 cells treated with D-mannose in the absence or presence of proteasome inhibitor MG132, or lysosome inhibitor NH4Cl, or autophagy inhibitor 3-MA. (*D*) Western blot analysis of PD-L1 ubiquitination level under D-mannose treatment in MDA-MB-231 cells stably expressing Flag-PD-L1. Ubiquitinated PD-L1 proteins were immunoprecipitated with Flag beads and blotted with HA antibody. (*E*) Western blot analysis of PD-L1 WT and NQ mutants in MDA-MB-231 cells treated with or without D-mannose. (*F*) Western blot analysis of PD-L1 as well as AMPK-α and p-AMPK-α in MDA-MB-231 cells treated with D-mannose for different time as indicated. (*G*) Western blot analysis of PD-L1 as well as AMPK-α and p-AMPK-α in MDA-MB-231 cells treated with different concentrations of D-mannose as indicated. (*H*) The effect of D-mannose on the interaction between PD-L1 and AMPK-α in MDA-MB-231 cells was determined by co-IP and Western blot. (*I*) The function of AMPK-α on D-mannose–induced PD-L1 degradation was determined by Western blot. AMPK-α WT and KO cells were treated with D-mannose (100 mM, 48 h). Levels of PD-L1 as well as AMPK-α and p-AMPK-α in MDA-MB-231 cells were examined by Western blot. (*J*) The effect of AMPK inhibition on D-mannose–induced PD-L1 degradation was determined by Western blot. MDA-MB-231 cells were pretreated with AMPK inhibitor dorsomorphin (10 μM, 6 h) before cells were treated with D-mannose (100 mM, 48 h). Levels of PD-L1 as well as AMPK-α and p-AMPK-α in MDA-MB-231 cells were examined by Western blot. (*K*) Western blot analysis of WT, S195A, S195D, and S195E mutants of PD-L1 in MDA-MB-231 cells. (*L*) Western blot analysis of WT, S195A, S195D, and S195E mutants of PD-L1 as well as AMPK-α and p-AMPK-α in MDA-MB-231 cells treated with or without D-mannose (100 mM, 48 h). (*M*) CHX-chase assay showing the degradation of PD-L1 WT and S195A mutant in MDA-MB-231 cells treated with D-mannose (100 mM, 48 h).

correlated with PD-L1 protein levels in a D-mannose treatment time– and dose–dependent manner (Fig. 2 *F* and *G*). Moreover, we assessed the binding of AMPK to PD-L1 in the absence and presence of D-mannose and found that D-mannose promoted the interaction between PD-L1 and AMPK (Fig. 2*H*). Furthermore, both genetic depletion and pharmacological inhibition of AMPK abolished the D-mannose–induced band shift and reduction of PD-L1 (Fig. 2 *I* and *J*). These results suggest that D-mannose may impair the glycan structure of PD-L1 through

AMPK-mediated phosphorylation. It has been reported that metformin can also promote abnormal glycosylation and band shift of PD-L1 via AMPK-mediated S195 phosphorylation (18), which phenocopies D-mannose treatment. To validate our hypothesis, we generated the PD-L1 phosphorylation site mutants S195A (nonphosphomimetic), S195E (phosphomimetic), and S195D (phosphomimetic) and assessed their band shifts by Western blot. Compared with WT PD-L1, the S195A mutant showed no band shift, while both the S195E and S195D

mutants showed a lower band similar to that seen under D-mannose treatment (Fig. 2K) (18). In addition, when treated with D-mannose, only WT PD-L1 decreased, and all three S195 mutants showed no response (Fig. 2L). In line with this finding, the nonphosphomimetic mutant S195A showed a longer half-life than WT PD-L1 under D-mannose treatment (Fig. 2M). We also utilized a pan-serine phosphorylation antibody to examine the p-Ser levels of WT and S195A mutant PD-L1 upon D-mannose treatment. S195 of PD-L1 locates between two N-glycosylation sites (N192 and N200), and it was reported that the glycans need to be removed to detect the S195 phosphorylation (18). Therefore, after immunoprecipitation (IP) purification of PD-L1, we treated the samples with PNGase F to remove glycans and the PD-L1 bands moved to ~35 kDa. Results showed that D-mannose treatment promoted the pan-serine phosphorylation of WT but not S195A mutant PD-L1 (*SI Appendix*, Fig. S2C). Together, these results suggest that D-mannose promotes the degradation of PD-L1 through AMPK-mediated phosphorylation, dysregulation of glycosylation, and ubiquitination.

To find out if it is a linear pathway or the phosphorylation of AMPK and glycosylation-Ub events are mutually exclusive, we treated cells with N-linked glycosylation inhibitor tunicamycin (TM) and examined the phosphorylation of AMPK and ubiquitination of PD-L1. Results showed that TM treatment inhibited PD-L1 glycosylation and hence promoted PD-L1 ubiquitination and proteasomal degradation (*SI Appendix*, Fig. S2A). Note that the phosphorylation level of AMPK had no response to TM treatment, indicating it is a linear pathway but not a mutually exclusive regulation, and the kinetic of Ub is directly regulated by glycosylation, rather than AMPK phosphorylation. Lastly, we determined whether it is a general mechanism that D-mannose–mediated degradation of proteins that are regulated by AMPK or glycosylation by examining the phosphorylation and protein levels of ACC and B7H3 under D-mannose treatment. ACC is a well-known target of AMPK; D-mannose promoted the phosphorylation of ACC but didn't decrease its protein level (*SI Appendix*, Fig. S2B). B7H3 is a highly glycosylated protein and has been reported to be stabilized by N-glycosylation (26). However, results showed that D-mannose caused a band shift of B7H3 protein but didn't reduce its protein level, suggesting the glycosylation of B7H3 may be impaired by D-mannose treatment but not enough to destabilize the protein (*SI Appendix*, Fig. S2B). Collectively, D-mannose may affect the phosphorylation levels of AMPK targets and glycosylation levels of glycoproteins but not always regulate their stability.

D-mannose Promotes T Cell Activation and T Cell Killing of TNBC Cells In Vitro. To test whether the abnormal PD-L1 glycosylation and PD-L1 degradation induced by D-mannose affects PD-1 binding, we incubated tumor cells with recombinant human PD-1 Fc chimera protein. Immunofluorescence assays revealed that D-mannose significantly decreased PD-1 binding to tumor cells (Fig. 3A). We next examined the effect of D-mannose pretreatment of tumor cells on T cell activation. We cocultured tumor cells with PHA-stimulated Jurkat T cells. The up-regulation of PD-1 validated the PHA-induced activation of Jurkat T cells (Fig. 3B), and coculture with MDA-MB-231 or BT-549 cells reduced IL-2 mRNA levels in activated Jurkat T cells, while these levels could be rescued by D-mannose treatment of tumor cells (Fig. 3C). Similar experiments were conducted with 4T1 mouse breast cancer cells. We first confirmed the effect of D-mannose on PD-L1 in 4T1 cells (Fig. 3D). Then, mouse-derived activated CD8+ T cells were cocultured with 4T1 cells with or without D-mannose pretreatment. The expression levels of IL-2 and IFN-γ in CD8+ T cells were measured. In line with previous results, the levels of IL-2 and IFN-

γ were reduced in CD8+ T cells cocultured with 4T1 cells, which could be reversed by D-mannose treatment of tumor cells (Fig. 3 E and F). Furthermore, we determined the effect of D-mannose on T cell–mediated tumor cell killing. Activated T cells (Fig. 3G) were cocultured with MDA-MB-231 cells with or without D-mannose pretreatment. The results showed that D-mannose pretreatment of tumor cells significantly enhanced the killing effect of T cells (Fig. 3H). Overall, D-mannose promoted T cell activation and T cell killing of tumor cells in vitro.

D-mannose Synergizes with Anti–PD-1 Antibody to Inhibit TNBC Cell Growth. It is well established that suppression of PD-L1 in tumor cells activates antitumor immunity. We next examined the role of D-mannose–down-regulated PD-L1 expression in tumor immune evasion in mice. 4T1 mouse breast cancer cells were inoculated into the mammary fat pad of BALB/c mice, and mice were treated with D-mannose and anti–PD-1 antibodies as indicated in Fig. 4A. Consistent with our observations in vitro, oral administration of D-mannose reduced tumor size and extended the survival of mice with a similar effect as the anti–PD-1 antibody, and importantly, the combination of D-mannose and anti–PD-1 antibody conferred the best efficacy (Fig. 4 B–D). Notably, ~40% of mice still survived 65 d postinoculation under treatment with D-mannose and anti–PD-1 antibodies, while mice treated with anti–PD-1 antibody alone all died within 41 d (Fig. 4D). Western blot analysis confirmed that oral administration of D-mannose decreased tumoral PD-L1 levels in mice (Fig. 4E). In addition, we determined whether macrophages respond to D-mannose like tumors. 4T1 model mice were divided into two groups, one fed with normal drinking water, and the other fed with water containing D-mannose. After 2-wk treatment, the expression level of PD-L1 on tumor-infiltrating macrophages was examined by flow cytometry (*SI Appendix*, Fig. S3A). Results showed that macrophages in 4T1 model did response to D-mannose like tumors and the expression of PD-L1 on macrophages decreased upon D-mannose treatment (*SI Appendix*, Fig. S3B). Furthermore, immunohistochemistry (IHC) staining of tumor tissues demonstrated that D-mannose increased the tumor-infiltrating CD8+ T cell population and granzyme B levels, and consistently, the combination of D-mannose and PD-1 blockade exhibited a significant synergetic effect in terms of stimulating tumor infiltration of CD8+ T cells and antitumor immunity (Fig. 4 F and G). Collectively, these in vivo data show that D-mannose have a similar effect as anti–PD-1 antibodies and, more importantly, can be used to enhance the efficacy of immune checkpoint blockade therapy.

D-mannose Inhibits the PD-L1–Mediated DDR and Sensitizes TNBC Cells to Ionizing Radiation (IR). A previous study discovered that intracellular PD-L1 can act as an RNA-binding protein and protect mRNAs of DDR-related genes from degradation, thus increasing the resistance of tumors to DNA damage (11). We next tested whether D-mannose treatment can regulate the mRNA levels of DDR-related genes through degradation of PD-L1. We found that D-mannose significantly decreased the mRNA and protein levels of BRCA1, RAD50, and MRE11 in both MDA-MB-231 and BT-549 cells (Fig. 5 A–D). Then, we assessed the impact of D-mannose on the mRNA stability of DDR-related genes. We treated MDA-MB-231 cells with the transcriptional inhibitor actinomycin D and determined the mRNA levels of BRCA1, RAD50, and MRE11 over time. The decay of their mRNAs was significantly faster in D-mannose–treated cells than in control cells (Fig. 5E). To further confirm this finding, PD-L1 was knocked out in MDA-MB-231 cells (Fig. 5F). We found that D-mannose treatment had no effect on the mRNA and protein levels of BRCA1, RAD50, and MRE11 in PD-L1 knockout (KO) cells (Fig. 5 G and H). Next, we assessed whether the DNA repair capacity of
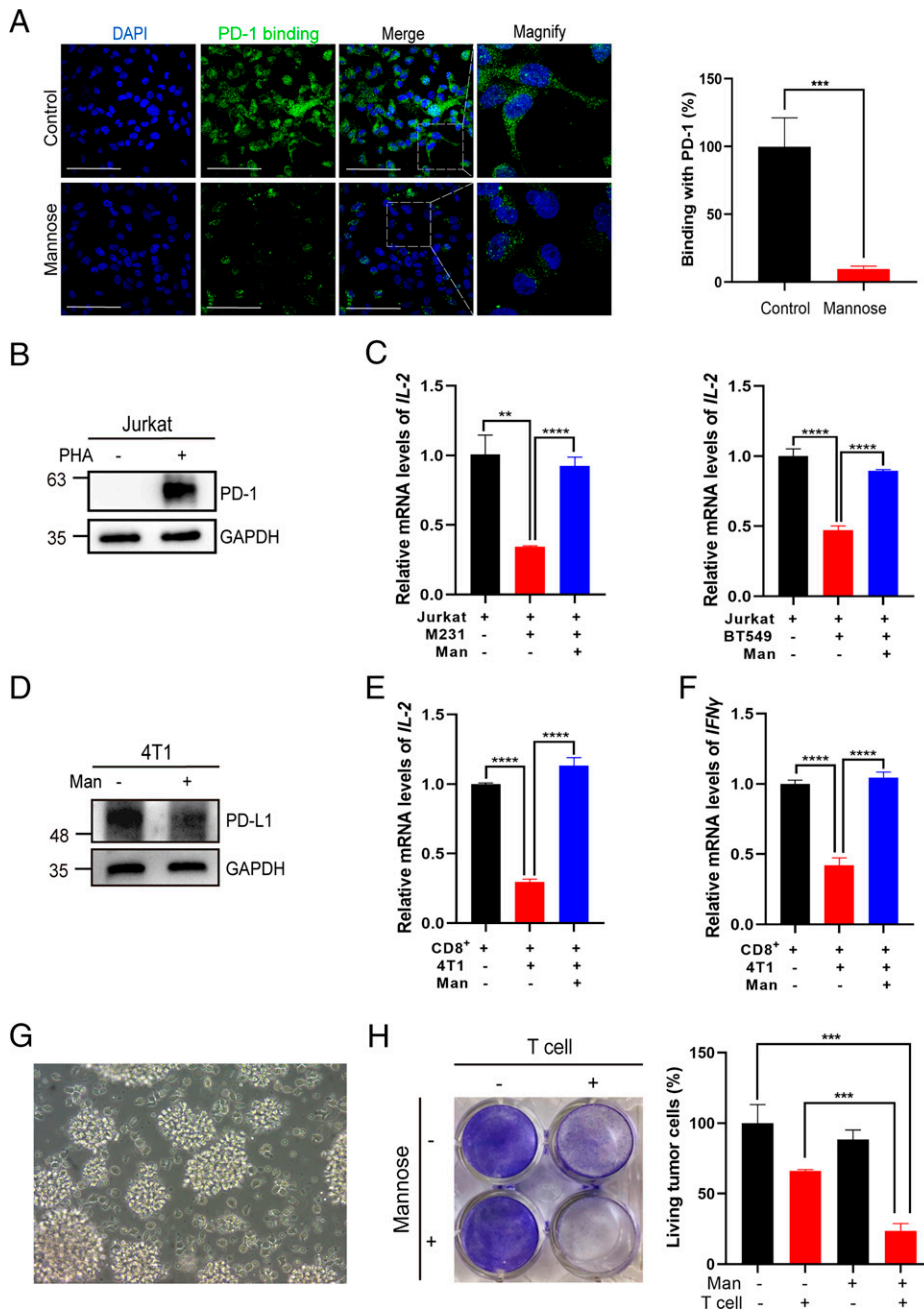
Zhang et al.
D-mannose facilitates immunotherapy and radiotherapy of triple-negative breast cancer via degradation of PD-L1

PNAS | 5 of 12
https://doi.org/10.1073/pnas.2114851119

Fig. 3. D-mannose promotes T cell activation and T cell killing of TNBC cells in vitro. (*A*) Immunostaining of PD-1 Fc chimera proteins on MDA-MB-231 cells treated with or without D-mannose (Scale bars, 100 μm). Quantitation of binding of PD-1/Fc were shown on the *Right*. Values are means ± SD from $n = 3$ independent experiments. Statistical differences were determined by Student's t test. ***$P < 0.001$. (*B*) Western blot analysis of PD-1 levels in Jurkat T cells stimulated with or without PHA for 72 h. (*C*) qRT-PCR analysis of IL-2 expression in Jurkat T cells cocultured with control or D-mannose–pretreated MDA-MB-231 or BT-549 cells. Jurkat T cells were activated by PHA and then cocultured with MDA-MB-231 or BT-549 cells pretreated with or without D-mannose. Values are means ± SD from $n = 3$ independent experiments. Statistical differences were determined by Student's t test. **$P < 0.01$, ***$P < 0.001$, ****$P < 0.0001$. (*D*) Western blot analysis of PD-L1 level in 4T1 mouse breast cancer cells treated with or without D-mannose. (*E*) qRT-PCR analysis of IL-2 expression in mouse primary CD8$^+$ T cells cocultured with control or D-mannose–pretreated 4T1 mouse breast cancer cells. Mouse primary CD8$^+$ T cells were preactivated with PMA and ionomycin and then cocultured with 4T1 mouse breast cancer cells pretreated with or without D-mannose. (*F*) qRT-PCR analysis of IFN-γ expression in mouse primary CD8$^+$ T cells cocultured with control or D-mannose–pretreated 4T1 mouse breast cancer cells. Mouse primary CD8$^+$ T cells were preactivated with PMA and ionomycin and then cocultured with 4T1 mouse breast cancer cells pretreated with or without D-mannose. Values are means ± SD from $n = 3$ independent experiments. Statistical differences were determined by Student's t test. ****$P < 0.0001$. (*G*) Morphology of activated human T cells. (*H*) The effect of D-mannose on T cell killing of TNBC cells was determined. Control and D-mannose–treated MDA-MB-231 cells were cocultured with activated T cell for 48 h and then subjected to crystal violet staining. The quantification was shown on the *Right*. Data represent mean ± SD $n = 3$. ***$P < 0.001$.

cancer cells could be compromised by D-mannose treatment. The phosphorylation of histone H2AX (γ-H2AX) is a marker of DNA double-strand breaks. MDA-MB-231 cells were subjected to IR, and then we used immunofluorescence to examine the kinetics of γ-H2AX foci in cells to determine DNA repair capacity. D-mannose–treated cells displayed delayed resolution of γ-H2AX foci, which indicated compromised DNA repair function (Fig. 5 *I* and *J*). Furthermore, the control and D-mannose–treated cells were subjected to IR and seeded into plates, and their colony formation ability was determined. The results showed that D-mannose–treated cells were more sensitive to IR and grew much slower than control cells (Fig. 5 *K* and *L*). Together, these results demonstrate that D-mannose can decrease the mRNA stability of BRCA1, RAD50, and MRE11 through degradation of PD-L1, therefore making tumor cells more sensitive to IR treatment.

D-mannose Sensitizes TNBC Cells to Radiotherapy. Our finding that D-mannose decreases the stability of mRNAs involved in DDR suggested that D-mannose may be a potential drug that can promote the efficacy of cancer radiotherapy. To test this hypothesis, 4T1 tumor-bearing mice were treated with D-mannose or IR alone, or a combination of D-mannose and IR as indicated in Fig. 6*A*. The results showed that D-mannose or IR alone had only moderate therapeutic effects, while the combination of D-mannose and IR dramatically inhibited tumor growth in mice (Fig. 6 *B–D*). Finally, we dissected the tumors from mice and provided in vivo evidence that D-mannose decreases PD-L1 expression levels (Fig. 6*E*) and boosts DNA damage in IR-treated tumors (Fig. 6*F*). The level of tumor-infiltrating CD8+ T cells was also determined by IHC staining, and results showed that both D-mannose alone and in combination with IR increased the tumor-infiltrating CD8+
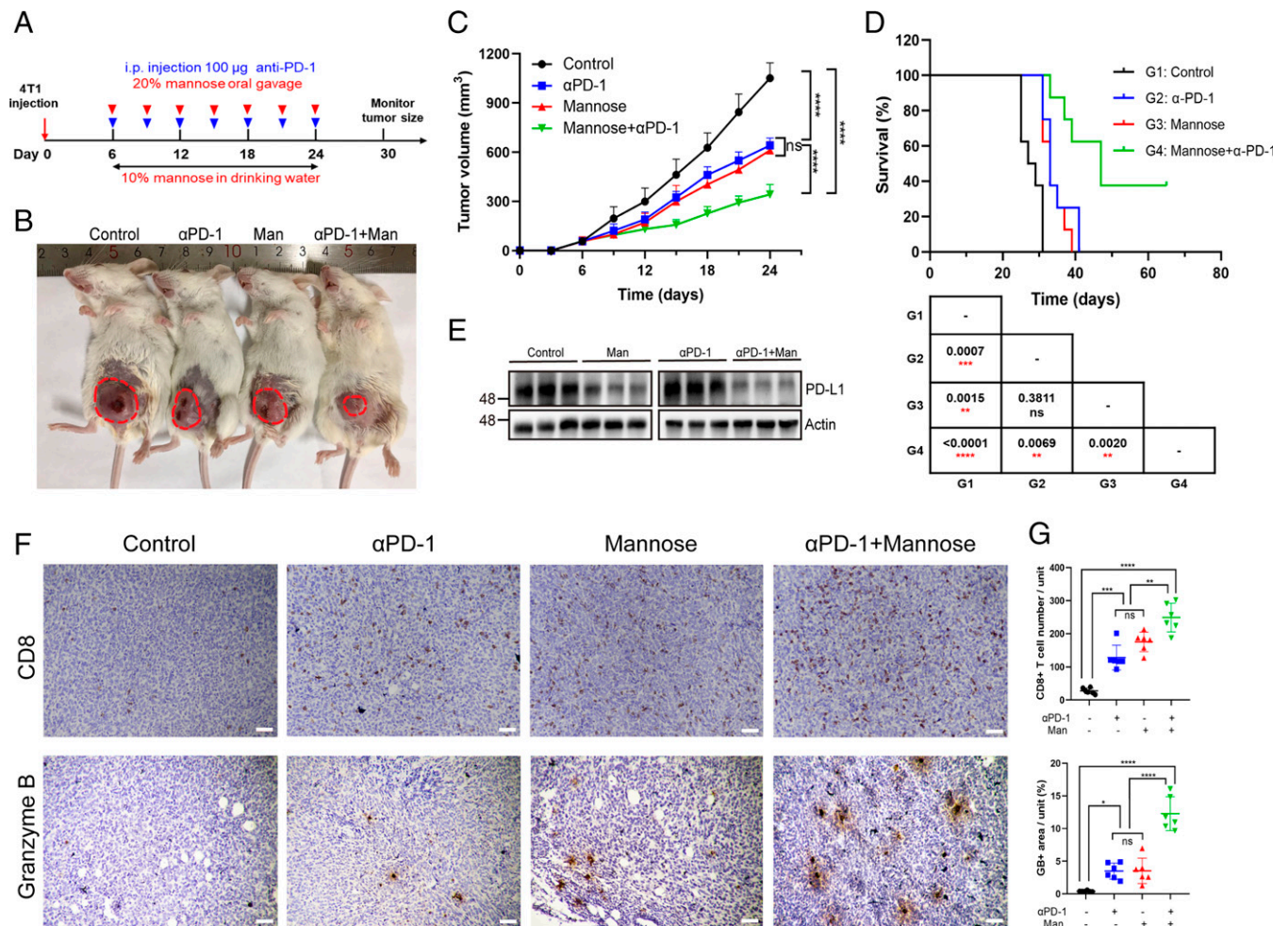
Fig. 4. D-mannose synergizes with PD-1 antibody to inhibit TNBC growth. (*A*) Schematic representation of the animal experiment process. (*B*) Representative tumors of 4T1 cells in BALB/c mice treated with D-mannose or/and anti–PD-1 antibody. (*C*) Tumor growth of 4T1 cells in BALB/c mice following treatment with D-mannose or/and anti–PD-1 antibody was determined. Tumors were measured at the indicated time points. $n = 8$ mice per group. Statistical differences were determined by ordinary one-way ANOVA. ns, no significance, ****$P < 0.0001$. (*D*) Kaplan–Meier survival curves for mice injected with 4T1 cells and treated with D-mannose or/and anti–PD-1 antibody. The *P* value, comparing every two groups, was determined using log-rank test and is shown in the table *Below* the figure. (*E*) Western blot analysis of PD-L1 level in 4T1 tumor tissues as indicated. (*F*) Immunohistochemistry showing CD8^{+} T cell infiltration and granzyme B expression in the 4T1 tumor tissues as indicated (Scale bars, 100 μm). (*G*) Quantifications of images in (*F*). Data represent mean ± SD from six independent samples of each group. Statistical differences were determined by ordinary one-way ANOVA. ns, no significance, *$P < 0.05$, **$P < 0.01$, ***$P < 0.001$, ****$P < 0.0001$.

T cells (*SI Appendix*, Fig. S4*A*). Collectively, D-mannose enhances the efficacy of radiotherapy via degradation of PD-L1 and up-regulation of IR-induced DNA damage.

Discussion

The function of glucose in cancer and immunity has been extensively investigated, while the role of other sugars in cancer immunity and treatment remains largely unexplored. In this study, we explored the function of D-mannose in immunotherapy and radiotherapy in TNBC, established a functional link between D-mannose and PD-L1, and provided a molecular mechanism through which D-mannose activates AMPK to phosphorylate PD-L1 at S195, leading to abnormal glycosylation and proteasomal degradation of PD-L1 (Figs. 2 and 7). Besides stabilizing PD-L1, N-linked glycosylation of PD-L1 is also required for its physical contact with PD-1 (27). In this study, D-mannose not only promotes degradation of PD-L1 but also induces abnormal glycosylation of residual PD-L1, both of which suppress the interaction of cell surface PD-L1 with PD-1. Based on these findings, we used D-mannose and anti–PD-1 antibodies to treat TNBC in

mice. The results showed that the combination of D-mannose with PD-1 blockade significantly suppressed TNBC growth and dramatically extended the lifespan of tumor-bearing mice (Fig. 4). In addition, D-mannose–induced PD-L1 degradation also results in mRNA destabilization of DDR-related genes (Fig. 5), thereby sensitizing breast cancer cells to IR treatment and facilitating radiotherapy of TNBC in mice (Figs. 6 and 7). Overall, our study discovered that D-mannose can significantly enhance immunotherapy and radiotherapy in TNBC. Whether D-mannose can induce PD-L1 degradation and facilitate immunotherapy and radiotherapy in other tumor types deserves further study.

Several PTMs have been reported to regulate the protein stability of PD-L1 (28). PD-L1 is heavily glycosylated, and glycosylation stabilizes PD-L1 and suppresses antitumor immunity (16), while the phosphorylation of PD-L1 by either GSK3-β or AMPK promotes its degradation (16, 18). Ubiquitylation (29–32) and palmitoylation (33, 34) also regulate PD-L1 stability. In this study, we found that D-mannose could induce abnormal glycosylation through AMPK-mediated phosphorylation, which promoted the ubiquitylation and degradation of PD-L1. The mechanism combines three different PTMs and is in line with other studies in
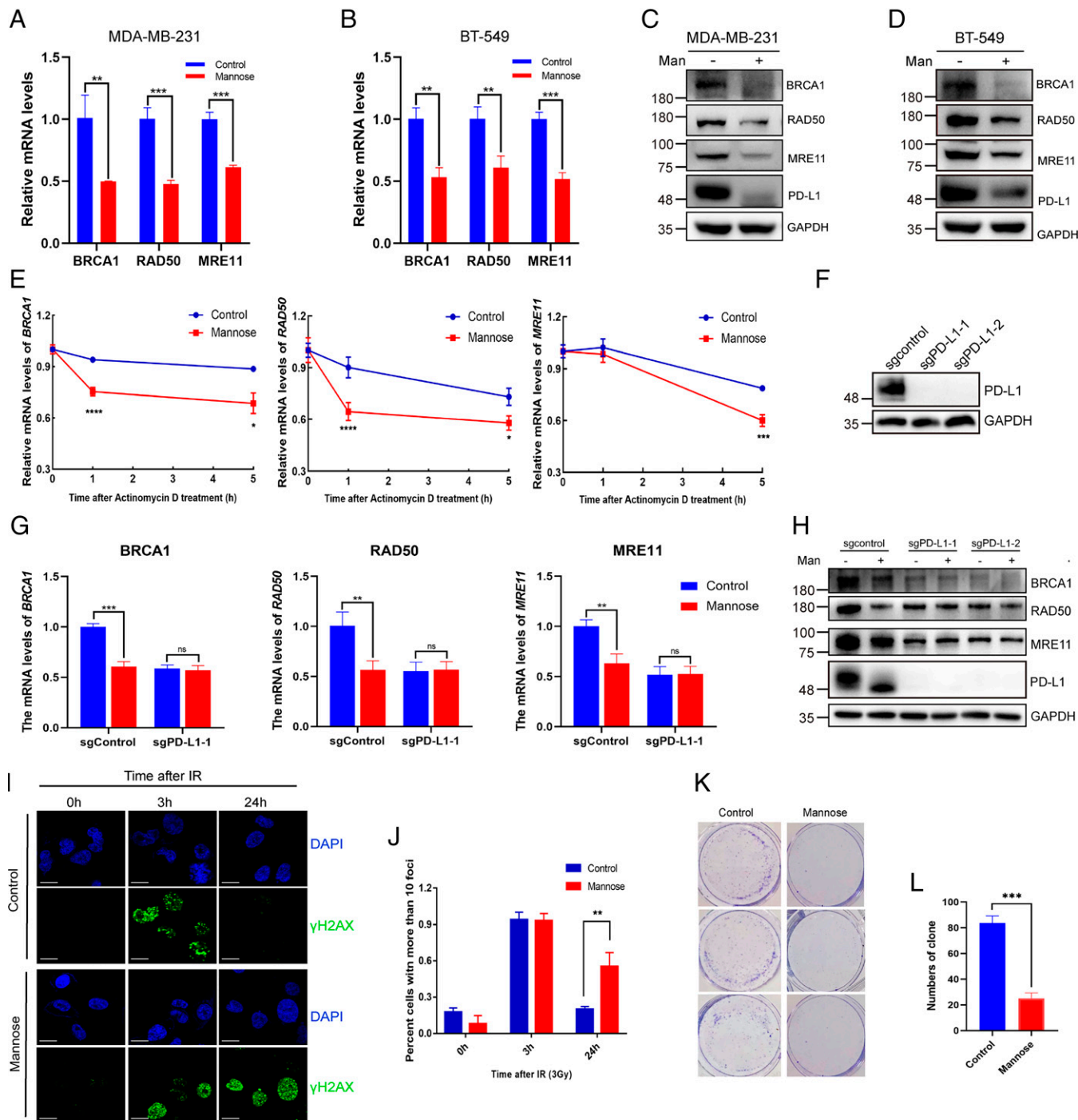
Zhang et al.
D-mannose facilitates immunotherapy and radiotherapy of triple-negative
breast cancer via degradation of PD-L1

PNAS | 7 of 12
https://doi.org/10.1073/pnas.2114851119

Fig. 5. D-mannose inhibits PD-L1–mediated DDR and sensitizes TNBC cells to IR. (*A* and *B*) qRT-PCR analysis of BRCA1, RAD50, and MRE11 mRNA levels under D-mannose treatment in MDA-MB-231 cells (*A*) and BT-549 cells (*B*). Values are means ± SD from *n* = 3 independent experiments. Statistical differences were determined by Student's *t* test. **P < 0.01, ***P < 0.001. (*C* and *D*) Western blot analysis of BRCA1, RAD50, and MRE11 levels in MDA-MB-231 cells (*C*) and BT-549 cells (*D*) treated with D-mannose. (*E*) qRT-PCR analysis of BRCA1, RAD50, and MRE11 mRNA levels in control and D-mannose–treated MDA-MB-231 cells after treating with the transcription inhibitor actinomycin D for different time as indicated. Values are means ± SD from *n* = 3 independent experiments. Statistical differences were determined by Student's *t* test. *P < 0.05, ***P < 0.001, ****P < 0.0001. (*F*) Western blot analysis of PD-L1 in control and PD-L1 KO MDA-MB-231 cells. (*G*) qRT-PCR analysis of BRCA1, RAD50, and MRE11 mRNA levels in control or PD-L1 KO MDA-MB-231 cells following D-mannose treatment. Values are means ± SD from *n* = 3 independent experiments. Statistical differences were determined by Student's *t* test. ns, no significance, **P < 0.01, ***P < 0.001. (*H*) Western blot analysis of BRCA1, RAD50, and MRE11 levels in control or PD-L1 KO MDA-MB-231 cells under D-mannose treatment. (*I*) Immunostaining of γ-H2AX in MDA-MB-231 cells with IR (3Gy) and D-mannose treatment as indicated. (*J*) Quantifications of images in (*I*). Data represent mean ± SD from three independent samples of each group. Statistical differences were determined by Student's *t* test. **P < 0.01. (*K*) The growth of control and D-mannose–treated MDA-MB-231 cells under IR (3Gy) treatment was determined by colony formation assay. (*L*) Quantifications of images in (*K*). Data represent mean ± SD. Statistical differences were determined by Student's *t* test. ***P < 0.001.

Zhang et al.
D-mannose facilitates immunotherapy and radiotherapy of triple-negative
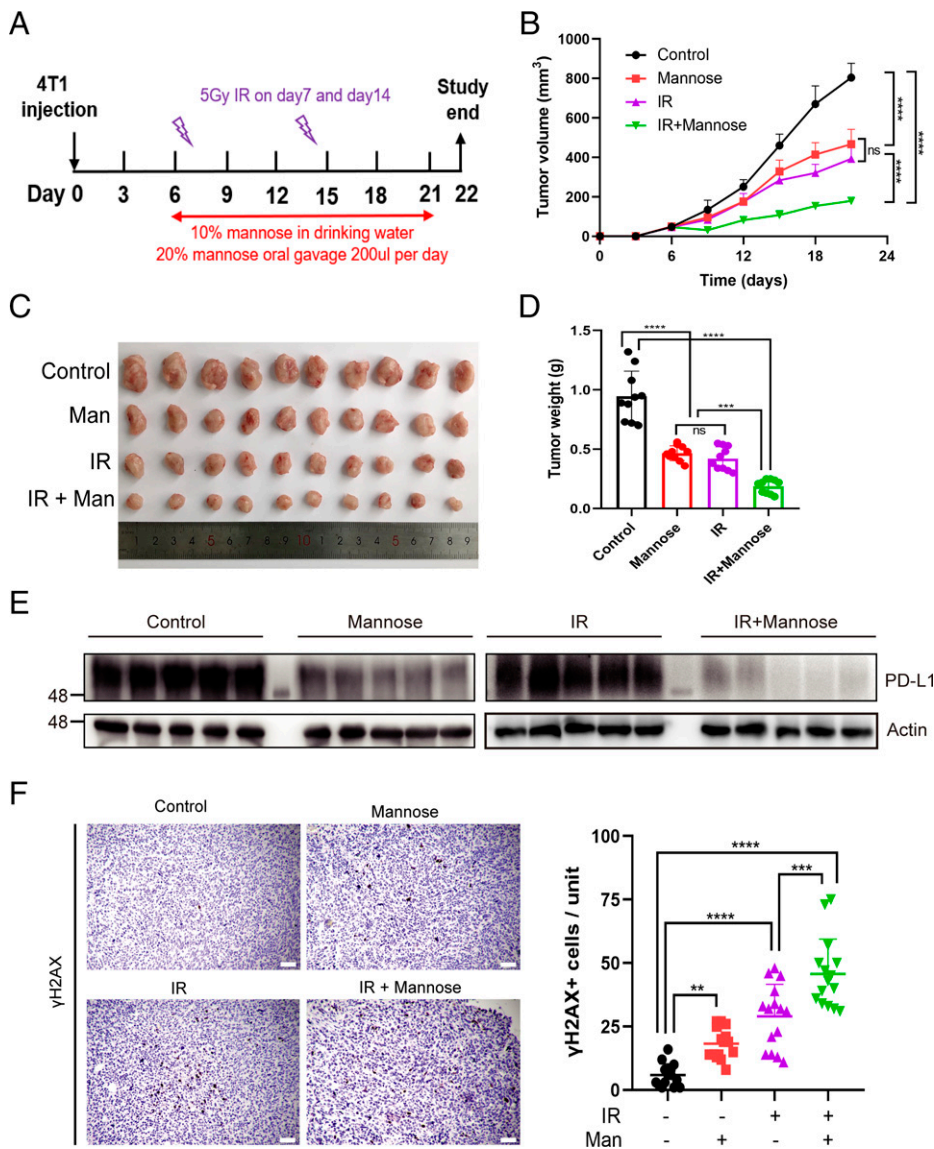breast cancer via degradation of PD-L1

Fig. 6. D-mannose sensitizes TNBC to radiotherapy. (*A*) Schematic representation of the animal experiment process. (*B*) Tumor growth of 4T1 cells in BALB/c mice treated with D-mannose or/and IR was determined. $n = 10$ mice per group. Statistical differences were determined by ordinary one-way ANOVA. ns, no significance, ****$P < 0.0001$. (*C*) Representative tumors resected from each group of mice that received different treatment as indicated. (*D*) The weight of tumors resected from each group of mice that received different treatment as indicated was analyzed. Data represent mean $\pm$ SD, $n = 10$ mice per group. Statistical differences were determined by ordinary one-way ANOVA. ns, no significance, ***$P < 0.001$, ****$P < 0.0001$. (*E*) Western blot analysis of PD-L1 level in 4T1 tumor tissues as indicated. (*F*) *Left*: Immunohistochemistry showing γ-H2AX expression in the 4T1 tumor tissues (Scale bars, 100 μm). *Right*: Quantifications of the immunohistochemistry images. Data represent mean $\pm$ SD from 15 independent samples of each group. Statistical differences were determined by ordinary one-way ANOVA. **$P < 0.01$, ***$P < 0.001$, ****$P < 0.0001$.

the field. Our study also suggests that D-mannose may promote the phosphorylation of multiple AMPK targets and regulate their functions.

It is surprising that D-mannose, as the major monosaccharide component of N-glycans, suppresses but not enhances glycosylation of PD-L1. Notably, the physiological concentration of D-mannose in human blood is ~50 μM, which is considered enough for protein N-glycosylation (23), suggesting D-Mannose is not a rate-limiting factor for protein glycosylation and exogenous D-mannose may have minor or no effect on stimulating PD-L1 glycosylation by providing monosaccharide. Indeed, we found that instead of stimulating glycosylation, supraphysiological levels of D-mannose reduces PD-L1 glycosylation through activation of AMPK and subsequent phosphorylation of PD-L1, leading to degradation of PD-L1. This finding also suggests that D-mannose may play an important role in regulation of other proteins' glycosylation. Given that glycosylation has profound structural and functional effects on glycoproteins, it would be worth examining the impact of D-mannose on other glycoproteins.

D-mannose is imported into mammalian cells via membrane glucose transporters and can be phosphorylated by HK to produce M6P. In PMI-low cells, M6P is accumulated and inhibits

the activity of glycolytic enzymes HK and PGI, thus impairing glycolysis (21, 23). Here, we found that MDA-MB-231 cells, which have been reported to possess high levels of PMI, showed glycolysis up-regulation in response to D-mannose treatment. Our finding provides an insight into how D-mannose is involved in glycolysis regulation; it would be interesting to further explore the function of D-mannose on metabolism in PMI-high cells. In addition to its effects on tumors, mannose may affect tumor microenvironment (TME) as well, which would also impact sensitivity of tumors to immune checkpoint inhibitors. We have shown that D-mannose decreased the expression of PD-L1 on tumor-infiltrating macrophages (*SI Appendix*, Fig. S3), which may exert synergetic antitumor effects. D-mannose was previously reported to increase the proportion of Foxp3+ regulatory T cells in mouse models of autoimmune diabetes and airway inflammation (22); whether D-mannose can act on the Treg cells in TME is worth exploring. It would also be interesting to determine whether D-mannose affects the metabolism and function of CD4+ and CD8+ T cells. Collectively, the function of D-mannose in TME and tumor immunity merits further exploration, which may uncover therapeutic windows to enhance the efficacy of immunotherapy.
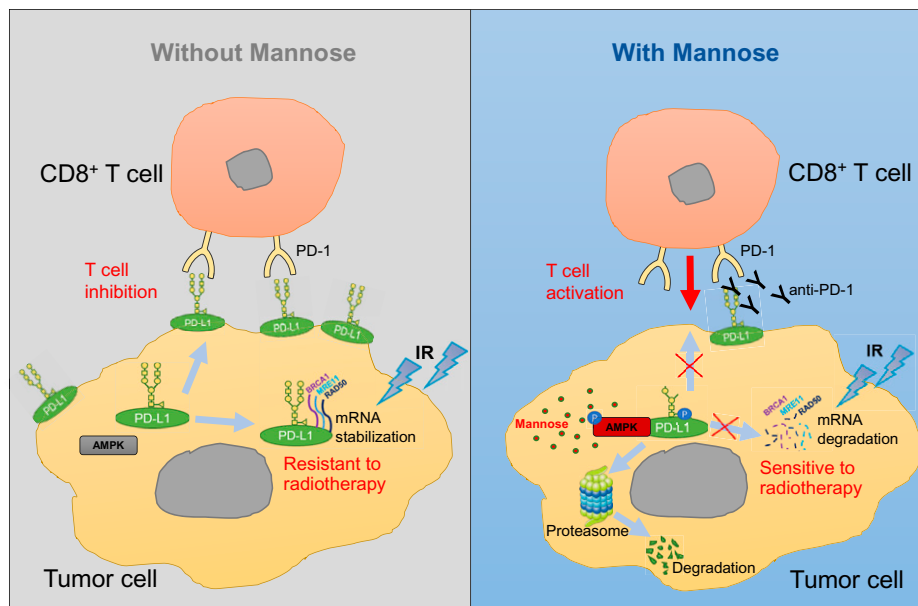
Zhang et al.
D-mannose facilitates immunotherapy and radiotherapy of triple-negative breast cancer via degradation of PD-L1

PNAS | 9 of 12
https://doi.org/10.1073/pnas.2114851119

Fig. 7. D-mannose induces PD-L1 abnormal glycosylation and degradation through proteasome, promoting cancer immunotherapy and radiotherapy. Membrane localized PD-L1 can interact with PD-1 on T cells to inhibit T cell activation. While intracellular PD-L1 can serve as an RNA-binding protein and stabilize the mRNAs of BRCA1, RAD50, and MRE11 to promote the DDR in tumor cells, which makes tumor cells resistant to IR treatment. Under D-mannose treatment, PD-L1 is phosphorylated by AMPK at S195, leading to its abnormal glycosylation and proteosomal degradation, which synergizes with anti–PD-1 antibody to promote T cell activation and facilitates mRNA decay of BRCA1, RAD50, and MRE11, thereby sensitizing tumor cells to immunotherapy and radiotherapy.

Currently, several clinical trials of anti–PD-L1 treatment in TNBC are showing encouraging and positive responses (35, 36). However, the patient response rate is low (10 to 20%), and many patients remain refractory despite tumors expressing PD-L1 (25). It would be an excellent opportunity to test D-mannose. As shown in Fig. 7, D-mannose induces PD-L1 abnormal glycosylation and degradation in cytoplasm, which suppresses PD-L1 supplementation to membrane, thus decreasing PD-L1 levels on the cell surface. Therefore, combination of D-mannose and anti–PD-1/PD-L1 not only cut down supplementation of membrane PD-L1 from cytoplasm but also abolished the function of residual PD-L1 on the cell surface, further enhancing the T cells' killing of tumor cells, which was supported by the increased CD8+ T cell infiltration and granzyme B expression in tumors (Fig. 4 F and G). These findings demonstrated that combination of D-mannose and anti–PD-1/PD-L1 or other immune checkpoint inhibitors is a promising treatment for TNBC patients, including refractory patients, and may increase the efficacy of immunotherapy and the response rate in TNBC. Importantly, the effective level of D-mannose, which has been proven to be well tolerated in mice (20–22), can be easily achieved via drinking-water supplementation in mice, indicating that oral administration of D-mannose can be a simple, safe, and effective treatment for TNBC. In addition, cranberry, previously reported to inhibit urinary tract infection caused by *Escherichia coli*, is a fruit rich in mannose (37). It will be interesting to examine the potential of cranberry to enhance immunotherapy and radiotherapy in TNBC.

In summary, our study established a functional link between a metabolite and immune evasion and uncovered an unknown effect of D-mannose on immunotherapy and radiotherapy of TNBC. The findings of this study pave the way for the potential use of D-mannose in the clinical treatment of TNBC.

Materials and Methods

Cell Culture and Transfection. Human breast cancer cell line MDA-MB-231 and 293T cells were cultured in Dulbecco's modified Eagle medium (DMEM) containing 10% fetal bovine serum (FBS) and 1% penicillin/streptomycin (P/S). Roswell Park Memorial Institute (RPMI) medium 1640 containing 10% FBS and 1% P/S were used to culture human breast cancer cell line BT-549 and mouse breast cancer cell line 4T1. For transfection, cells were transfected with plasmids using EZ-trans (Life-iLab). To package lentivirus, the LentiCRISPRv2 KO constructs were transfected into 293T cells with packaging plasmids. Cell culture medium was changed 8 h posttransfection, and supernatant was collected twice with 24-h intervals. The supernatant was filtered using a 0.45-μm filter. The target cells were incubated in lentivirus-containing medium with polybrene (10 μg/mL) for 48 h and then subjected to puromycin selection.

DNA Constructs and Mutagenesis. Human CD274 (PD-L1) gene was cloned into pLVX-2Flag lentiviral expression vector, and Flag-PD-L1–expressed stable cell lines were established. Different mutants of PD-L1 were generated by site-directed mutagenesis PCR using KOD Fx (TOYOBO) according to the product manual. PD-L1 plasmids were amplified with mutation specific primers for 30 cycles, and the products were digested with DpnI enzyme (Takara) to eliminate template DNA, transformed into NcmDH5-α component cells (NCM Biotech), and plated on ampicillin-containing culture media. The incorporation of designed mutation was confirmed by sequencing of different clones. Deletion of PD-L1 was achieved by the CRISPR/Cas9 system, using LentiCRISPRv2 vector. The guide RNA sequences targeting PD-L1 were as follow: GTTCCCAAGGACC-TATATG; GAACATGAACTGACATGTC. Deletion of AMPK-α was conducted following the method previously described (18).

qRT-PCR Analysis. Total RNA was extracted using EZ-press RNA Purification Kit (EZBioscience). The complementary DNA was synthesized from purified RNA using 4×Reverse Transcription Master Mix (EZBioscience) according to the manufacturer's instructions. qRT-PCR was performed using an Applied Biosystem 7300 plus Sequence Detection System (Applied Biosystems). The cycle threshold (Ct) values were analyzed using the $2^{-\Delta\Delta Ct}$ method, and the final results were presented as relative fold change. The expression of Actin served as internal reference. The sequences of primers used for qRT-PCR are shown in Table 1.

Liquid Chromatography–Mass Spectrometry Analysis of Glycolytic Metabolites. MDA-MB-231 cells were treated with D-mannose for 72 h, and the cold methanol solution (80% vol/vol) was used to stop cell metabolism quickly. Then, samples were freeze-thawed five times in liquid nitrogen and centrifuged for 15 min at $15,000 \times g$ at 4 °C to collect the supernatants. The supernatants were then lyophilized and reconstituted in 500 μL methanol/water (10:90 vol/vol). The separated metabolites were acquired using AB sciex6500 QTRAP System.

Western Blot and Coimmunoprecipitation. Cells were washed with phosphate-buffered saline (PBS) and lysed in Nonidet P-40 lysis buffer containing 1% protease inhibitor and 1% phosphatase inhibitor at 4 °C for 30 min. The

Zhang et al.
D-mannose facilitates immunotherapy and radiotherapy of triple-negative
breast cancer via degradation of PD-L1

Table 1. Primers used for qRT-PCR analysis

Primers	Forward 5′-3	Reverse 5′-3
hActin	GGCATAGAGGTCTTTACGGATGTC	TATTGGCAACGAGCGGTTCC
hPD-L1	TGGCATTTGCTGAACGCATTT	TGCAGCCAGGTCTAATTGTTTT
hBRCA1	ACCTTGGAACTGTGAGAACTCT	TCTTGATCTCCCACACTGCAATA
hRAD50	TACTGGAGATTTCCCTCCTGG	AGACTGACCTTTTCACCATGC
hMRE11	GGGGCAGATGCACTTTGTG	GAAGCAAAACCGGACTAATGTCT
hIL-2	GAATGGAATTAATAATTACAAGAATCCC	TGTTTCAGATCCCTTTAGTTCCAG
hIFNγ	TCGGTAACTGACTTGAATGTCCA	TCGCTTCCCTGTTTTAGCTGC
mIL-2	GTGCTCCTTGTCAACAGCG	GGGGAGTTTCAGGTTCCTGTA
mIFNγ	GCCACGGCACAGTCATTGA	TGCTGATGGCCTGATTGTCTT

cell lysates were heated with sodium dodecyl sulphate–polyacrylamide gel electrophoresis (SDS-PAGE) sample loading buffer at 95 °C for 15 min and subjected to Western blot analysis. For coimmunoprecipitation, the cell lysates were collected and centrifuged (12,000 rpm, 15 min, 4 °C), then the supernatants were incubated with anti-FLAG beads (AbHO) overnight at 4 °C. The beads were washed three times with Nonidet P-40 buffer, heated with SDS-PAGE sample loading buffer, and subjected to Western blot analysis. The Western blot was performed according to standard protocol. All commercial antibodies were diluted and used according to the manufacturer's instructions, as shown in Table 2.

Detection of Cell Surface PD-L1. The protocol for detecting cell surface PD-L1 has been described previously (38). After treatment of D-mannose for 72 h, cells were washed with PBS and transfered into different centrifuge tubes. Next, cells were incubated with allophycocyanin (APC)-conjugated anti-human CD274 antibody (1:100) (BioLegend) on ice for 30 min in the dark. Then, cells were washed three times with 2 mL Cell Staining Buffer (BioLegend). Finally, the stained cells were analyzed by BD FACSCelesta (BD Biosciences) after resuspension with 200 μL staining buffer. Data were processed by FlowJo.

Immunofluorescence. Cells seeded in culture slides were washed twice with PBS and then fixed with 4% paraformaldehyde at room temperature (RT) for 15 min. For detecting the cytoplasm and nuclear proteins, cells were permeabilized in 0.5% Triton X-100 for 10 min. Then, cells were blocked in blocking solution containing bovine serum albumin for 1 h at RT and incubated with primary antibody γ-H2AX (Cell Signaling Technology) at 4 °C overnight, followed by secondary antibody Alexa Fluor 488–labeled Goat Anti-Rabbit IgG(H+L) (Beyotime Biotechnology) incubating for 1 h at RT. After nuclear staining using 4′,6-diamidino-2-phenylindole (DAPI), the slides were treated with antifade reagent and sealed by a coverslip. Finally, the slides were observed using Leica CTR6000 confocal microsystems.

Immunohistochemistry. Mouse 4T1 tumor sections were deparaffinized by deparaffinization buffer (Solarbio life science). Improved Citrate Antigen Retrieval Solution (Beyotime Biotechnology) and endogenous peroxidase

blocking buffer (Beyotime Biotechnology) were used for antigen retrieval and elimination of endogenous peroxidase activity, respectively. Then, the sections were blocked with goat serum in PBS for 30 min followed by incubating with antibodies at 4 °C overnight. After washing three times with PBS, tissues were incubated with horseradish peroxidase (HRP)-conjugated secondary antibodies, and DAB (3,3′-diaminobenzidine) HRP Color Development Kit was used for visualization. The commercially purchased antibodies used for IHC staining are shown in Table 3.

PD-L1 and PD-1 Binding Assay. The PD-1 binding assay was previously described (18). Briefly, MDA-MB-231 cells were seeded in culture slides, fixed in 4% paraformaldehyde at RT for 15 min, and then incubated with recombinant human PD-1 Fc protein (R&D Systems) for 1 h. Anti-human Alexa Fluor 488 dye conjugate (Life Technologies) was used as secondary antibody. Nuclei were stained with DAPI. After treating with antifade reagent and sealing by coverslips, the slides were observed using Leica CTR6000 confocal microsystems.

Coculture Experiments. The protocol for coculture experiments has been described previously (39). Mouse primary CD8+ T cells were isolated form the spleen of mice using the Ms CD8a IMag Particles (BD Pharmingen) following the manufacture's protocol. Mouse primary CD8+ T cells were activated with phorbol 12-myristate 13-acetate (PMA) (50 ng/mL, MedChemExpress) and ionomycin (500 ng/mL, MedChemExpress) for 12 h and then cocultured with 4T1 cells. Jurkat T cells were activated with PHA (500 ng/mL) for 72 h and then cocultured with MAD-MB-231 or BT-549 cells. After coculture, the T cells were collected and subjected to RNA extraction and qRT-PCR analysis.

T Cell–Mediated Tumor Cell Killing Assay. Human peripheral blood mononuclear (PBMC) cells were isolated from the blood of healthy donor. To acquire activated T cells, PBMCs were activated by ImmunoCult Human CD3/CD28/CD2 T cell activator (25 μL/mL, Stemcell) in the first 3 d and cultured in ImmunoCult-XF T cell expansion medium (Stemcell) supplemented with IL-2 (10 ng/mL, Pepro Tech) for 7 d according to the manufacturer's protocol. MDA-MB-231 cells were pretreated with mannose for 3 d, then the control and mannose treated cells were allowed to adhere to the plates overnight. After that, the activated T cells were cocultured with the tumor cells at a ratio of 10:1 in the DMEM/F12 medium containing 10% FBS and 1% P/S, supplemented with anti-CD3 antibody (100 ng/mL, eBioscience, Thermo Scientific) and IL-2 (10 ng/mL) for 48 h. Cell debris were removed by PBS wash, and living cancer cells were subjected to crystal violet staining and then washed with 33% (vol/vol) acetic acid followed by quantification using a spectrometer at optical density 570 nm.

Animal Experiments. All animal experiments were executed in accordance with the ethical obligations approved by the department of laboratory animal science of Fudan University. BALB/C mice (6- to 8-wk-old female) were purchased from JieSiJie Laboratory Animals. 4T1 cells (1×10^5 cells) were implanted into the mammary fat pad of mice, and PD-1 antibodies (100 μg) were injected intraperitoneally. For mannose treatment, mice were given 10% (m/v) mannose in drinking water and 200 uL 20% (m/v) mannose by oral

Table 2. Antibodies used for Western blot

Antibody	Source	Category No.
human PD-L1	Cell Signaling Technology	51296
GAPDH	Proteintech	60004-1-Ig
Alix	Huabio	ET1705-74
TSG101	Huabio	ET1701-59
Flag-tag	AbHO	HOA012FL01
AMPK-α	Cell Signaling Technology	5831
p-AMPK-α (Thr172)	Cell Signaling Technology	2535
PD-1	Cell Signaling Technology	86163
mouse PD-L1	Bio X Cell	BE0101
BRCA1	Absci	AB21234
RAD50	KleanAB	P100993
MRE11	KleanAB	P102335
γ-H2AX	Cell Signaling Technology	9718
Phosphoserine	Abcam	ab9332
B7H3	Cell Signaling Technology	14058T
ACC	Cell Signaling Technology	3676T
p-ACC (Ser79)	Cell Signaling Technology	11818T

Table 3. Antibodies used for IHC staining

Antibody	Source	Category No.
γ-H2AX	Cell Signaling Technology	9718
CD8-α	Cell Signaling Technology	98941
Granzyme B	Cell Signaling Technology	ab255598

gavage daily. Tumors were measured every 3 d with a caliper, and tumor volume was calculated using the formula: $\pi / 6 \times \text{length} \times \text{width}^2$. Mice were euthanized when tumors reached 1,500 mm^3.

Analysis of PD-L1 on Tumor-Infiltrating Macrophages. Tumors were digested to single cell suspension with Type IV collagenase (Sigma-Aldrich). Mouse Tumor-infiltrating lymphocyte Isolation Kit (Solarbio) was used to remove cancer cells and enrich leukocytes. Peridinin-chlorophyll-protein anti-mouse CD45 antibody (Biolegend) was used to mark the leukocytes. APC anti-mouse F4/80 (Biolegend) and fluorescein isothiocyanate anti-mouse/human CD11b (Biolegend) antibodies were used to mark macrophages. Phycoerythrin anti-mouse CD274 antibody (Biolegend) was used to detect the expression of PD-L1. Stained cells were analyzed by BD FACSCelesta (BD Biosciences). Data were processed by FlowJo.

Statistics. Statistical analysis was performed using GraphPad Prism 8 software. Data of bar graphs represents as fold change or percentage relative to control with SD of three independent experiments. Normally distributed data were analyzed using Student's t test. One-way ANOVA with Tukey's multiple comparisons was used when more than two groups were analyzed. Log-rank test was used for the mouse survival assay. Statistical significance was defined as $P < 0.05$. Levels of significance were indicated as $*P < 0.05$, $**P < 0.01$, $***P < 0.001$, and $****P < 0.0001$.

1. N. Harbeck *et al.*, Breast cancer. *Nat. Rev. Dis. Primers* **5**, 66 (2019).
2. A. G. Waks, E. P. Winer, Breast cancer treatment: A review. *JAMA* **321**, 288–300 (2019).
3. H. Katz, M. Alsharedi, Immunotherapy in triple-negative breast cancer. *Med. Oncol.* **35**, 13 (2017).
4. L. Yin, J. J. Duan, X. W. Bian, S. C. Yu, Triple-negative breast cancer molecular subtyping and treatment progress. *Breast Cancer Res.* **22**, 61 (2020).
5. M. Y. He *et al.*, Radiotherapy in triple-negative breast cancer: Current situation and upcoming strategies. *Crit. Rev. Oncol. Hematol.* **131**, 96–101 (2018).
6. G. J. Freeman *et al.*, Engagement of the PD-1 immunoinhibitory receptor by a novel B7 family member leads to negative regulation of lymphocyte activation. *J. Exp. Med.* **192**, 1027–1034 (2000).
7. H. Dong *et al.*, Tumor-associated B7-H1 promotes T-cell apoptosis: A potential mechanism of immune evasion. *Nat. Med.* **8**, 793–800 (2002).
8. D. M. Pardoll, The blockade of immune checkpoints in cancer immunotherapy. *Nat. Rev. Cancer* **12**, 252–264 (2012).
9. F. S. Hodi *et al.*, Improved survival with ipilimumab in patients with metastatic melanoma. *N. Engl. J. Med.* **363**, 711–723 (2010).
10. J. R. Brahmer *et al.*, Safety and activity of anti-PD-L1 antibody in patients with advanced cancer. *N. Engl. J. Med.* **366**, 2455–2465 (2012).
11. X. Tu *et al.*, PD-L1 (B7-H1) competes with the RNA exosome to regulate the DNA damage response and can be targeted to sensitize to radiation or chemotherapy. *Mol. Cell* **74**, 1215–1226.e4 (2019).
12. D. Shental-Bechor, Y. Levy, Effect of glycosylation on protein folding: A close look at thermodynamic stabilization. *Proc. Natl. Acad. Sci. U.S.A.* **105**, 8256–8261 (2008).
13. A. Varki, Biological roles of glycans. *Glycobiology* **27**, 3–49 (2017).
14. K. T. Schjoldager, Y. Narimatsu, H. J. Joshi, H. Clausen, Global view of human protein glycosylation pathways and functions. *Nat. Rev. Mol. Cell Biol.* **21**, 729–749 (2020).
15. N. Cherepanova, S. Shrimal, R. Gilmore, N-linked glycosylation and homeostasis of the endoplasmic reticulum. *Curr. Opin. Cell Biol.* **41**, 57–65 (2016).
16. C.-W. Li *et al.*, Glycosylation and stabilization of programmed death ligand-1 suppresses T-cell activity. *Nat. Commun.* **7**, 12632 (2016).
17. C. W. Li *et al.*, Eradication of triple-negative breast cancer cells by targeting glycosylated PD-L1. *Cancer Cell* **33**, 187–201.e10 (2018).
18. J. H. Cha *et al.*, Metformin promotes antitumor immunity via endoplasmic-reticulum-associated degradation of PD-L1. *Mol. Cell* **71**, 606–620.e7 (2018).
19. V. Sharma, H. H. Freeze, Mannose efflux from the cells: A potential source of mannose in blood. *J. Biol. Chem.* **286**, 10193–10200 (2011).
20. V. Sharma, M. Ichikawa, H. H. Freeze, Mannose metabolism: More than meets the eye. *Biochem. Biophys. Res. Commun.* **453**, 220–228 (2014).
21. P. S. Gonzalez *et al.*, Mannose impairs tumour growth and enhances chemotherapy. *Nature* **563**, 719–723 (2018).
22. D. Zhang *et al.*, D-mannose induces regulatory T cells and suppresses immunopathology. *Nat. Med.* **23**, 1036–1045 (2017).
23. S. Torretta *et al.*, D-mannose suppresses macrophage IL-1β production. *Nat. Commun.* **11**, 6343 (2020).
24. J. Wang *et al.*, d-mannose suppresses oxidative response and blocks phagocytosis in experimental neuroinflammation. *Proc. Natl. Acad. Sci. U.S.A.* **118**, e2107663118 (2021).
25. B. Shao *et al.*, Deglycosylation of PD-L1 by 2-deoxyglucose reverses PARP inhibitor-induced immunosuppression in triple-negative breast cancer. *Am. J. Cancer Res.* **8**, 1837–1846 (2018).
26. Y. Huang *et al.*, FUT8-mediated aberrant N-glycosylation of B7H3 suppresses the immune response in triple-negative breast cancer. *Nat. Commun.* **12**, 2672 (2021).
27. Y. N. Wang, H. H. Lee, J. L. Hsu, D. Yu, M. C. Hung, The impact of PD-L1 N-linked glycosylation on cancer therapy and clinical diagnosis. *J. Biomed. Sci.* **27**, 77 (2020).
28. J. H. Cha, L. C. Chan, C. W. Li, J. L. Hsu, M. C. Hung, Mechanisms controlling PD-L1 expression in cancer. *Mol. Cell* **76**, 359–370 (2019).
29. M. L. Burr *et al.*, CMTM6 maintains the expression of PD-L1 and regulates anti-tumour immunity. *Nature* **549**, 101–105 (2017).
30. R. Mezzadra *et al.*, Identification of CMTM6 and CMTM4 as PD-L1 protein regulators. *Nature* **549**, 106–110 (2017).
31. J. Zhang *et al.*, Cyclin D-CDK4 kinase destabilizes PD-L1 via cullin 3-SPOP to control cancer immune surveillance. *Nature* **553**, 91–95 (2018).
32. S. O. Lim *et al.*, Deubiquitination and stabilization of PD-L1 by CSN5. *Cancer Cell* **30**, 925–939 (2016).
33. Y. Yang *et al.*, Palmitoylation stabilizes PD-L1 to promote breast tumor growth. *Cell Res.* **29**, 83–86 (2019).
34. H. Yao *et al.*, Inhibiting PD-L1 palmitoylation enhances T-cell immune responses against tumours. *Nat. Biomed. Eng.* **3**, 306–317 (2019).
35. L. A. Emens, Immunotherapy in triple-negative breast cancer. *Cancer J.* **27**, 59–66 (2021).
36. T. E. Keenan, S. M. Tolaney, Role of immunotherapy in triple-negative breast cancer. *J. Natl. Compr. Canc. Netw.* **18**, 479–489 (2020).
37. Z. Wei, L. Huang, L. Cui, X. Zhu, Mannose: Good player and assister in pharmacotherapy. *Biomed. Pharmacother.* **129**, 110420 (2020).
38. H. B. Wang *et al.*, HIP1R targets PD-L1 to lysosomal degradation to alter T cell-mediated cytotoxicity. *Nat. Chem. Biol.* **15**, 42–50 (2019).
39. L. Du *et al.*, β-Catenin induces transcriptional expression of PD-L1 to promote glioblastoma immune evasion. *J. Exp. Med.* **217**, e20191115 (2020).

12 of 12 | **PNAS**
https://doi.org/10.1073/pnas.2114851119

Zhang et al.
D-mannose facilitates immunotherapy and radiotherapy of triple-negative breast cancer via degradation of PD-L1